International Journal of Engineering Technology Science and Research
IJETSR
www.ijetsr.com
ISSN 2394 – 3386
Volume 5, Issue 1
January 2018

Performance Analysis of Solar Air Heater Duct Roughened With Inclined Ribs with and without a Gap in a Staggered Roughness Arrangement on Absorber Plate

Mukesh Kumar Solanki[1*]
[1*]Research Scholar, Department of Mechanical Engineering, M.A.N.I.T. (MP), India
Dr. K. R. Aharwal[2]
[2]Associate Professor, Department of Mechanical Engineering, M.A.N.I.T. (MP) ,India

ABSTRACT

An experimental study has been conducted to investigate heat transfer, friction factor and thermo hydraulic performance characteristics of flow in a rectangular duct artificially roughened on inclined ribs with and without a gap in a staggered roughness arrangement on absorber plate. The rectangular duct has width to height ratio (W/H) of 8.0 and the Reynolds number based upon the mass flow rate of air at inlet of the duct ranged from 3000 to 14,000. The rib pitch-to height (P/e) ratio of 8, rib height-to-hydraulic diameter (e/ Dh) ratio of 0.045 and angle of attack (a) of 90°, relative gap position (dt/W & dl/W) of 0.3 & 0.1 and relative gap width (g/e) of 1.0. The maximum enhancement in Nusselt number (Nu) and friction factor (f) is observed to be 1.55 and 1.68 times of that of the smooth duct, respectively. The thermo-hydraulic performance parameter is found to be the maximum for the relative gap position (dt/W& dl/W) of 0.3 & 0.1 and the relative gap width of 1.0.

KEYWORDS: - Reynolds number (Re), Nusselt number, (Nu), Friction factor ((f), Relative gap width (g/e), Relative Gap position (dt/W& dl/W) and thermo hydraulic performance (Thp).

1. INTRODUCTION

In the present scenario of increasing energy demand and depleting fossil fuel solar energy has the potential of filling the gap of increasing energy demand. The energy required for various applications can be fulfilled by capturing solar energy efficiently. The most prolific way of utilizing solar energy is the conversion of it into thermal energy with the help of solar collectors. The solar air heater is not efficient due to low convective heat transfer coefficient between absorber plate and air. By providing artificial roughness on the underside of the absorber plate, heat transfer can be increased to make the system more effective. The investigation of enhancing heat transfer by using artificial roughness in solar air heaters has been carried out by several investigators in various energy fields. Varun et al. [1] carried out experimental investigations, using the combination of inclined and transverse wire ribs on the principal wall i.e. on the absorber plate of the solar air heater. Kumar et al. [2] investigated the effect of gap in the multiple V-ribs by the experimental investigations and found 6.74 times enhancement in Nusselt number and 6.37 times enhancement in friction factor over the smooth plate solar air heater. Prasad et al. [3] analytically investigated the effect of transverse circular wire ribs as artificial roughness by employing it on the three-sides of the solar air heater duct, and found it better than the one sided transverse ribs. Gupta et al. [4] found that inclined continuous ribs as roughness elements delivered higher thermal performance as compared to transverse and smooth plate solar air heater duct; they also evaluated the thermo hydraulic (effective) efficiency criteria analytically. Effective and thermal efficiency factor of discrete V-down roughness ribs was investigated by Singh et al. [5] by employing mathematical model. Mittal et al. [6] studied numerically the effective efficiency of five different roughness geometries and compared with the conventional solar air heater. The second law based analysis and entropy generation number of chamfered rib-groove rib roughened absorber plate

International Journal of Engineering Technology Science and Research
IJETSR
www.ijetsr.com
ISSN 2394 – 3386
Volume 5, Issue 1
January 2018

solar air heaters has been reported by Layek et al. [7]. Gupta et al. [8] studied numerically the energy, effective and exergy performance evaluation of solar air heater duct provided with different artificial roughness geometries. Gupta et al. [9] carried out there analytical investigation by using expanded metal mesh as roughness geometry of solar air heater duct; they evaluated the energy, effective and exergy augmentation criteria of the roughened duct. Lau et al. [10, 11] investigated the heat-transfer and friction factor characteristics of fully developed flow in a square duct with transverse and inclined discrete ribs. They reported that a five-piece discrete rib with 90° angle of attack shows 10–15% higher heat-transfer coefficient as compared to the 90° continuous ribs, whereas inclined discrete ribs give 10–20% higher heat transfer than that of the 90° discrete rib. Han et al. [12] carried out experiments to study the heat transfer and pressure drop characteristics of a roughened square channel with V-shaped broken rib arrangement with the angle of attack of 45° and 60° and reported that 60° V-shaped broken rib arrangement gives better performance than 45° V-shaped broken rib arrangement. Zhang et al. and Kiml et al. [12, 13] reported that the thermal performance of rib arrangements with an angle of attack of 60° is better than that with an angle of 45°, for a square duct. Chao et al. [14] examined the effect of angle of attack and number of discrete ribs, and reported that the gap region between the discrete ribs accelerates the flow, which increases the local heat-transfer coefficient. Cho et al. [15] investigated the effect of a gap in the inclined ribs on heat transfer in a square duct and reported that a gap in the inclined rib accelerates the flow and enhances the local turbulence, which will result in an increase in the heat transfer. They reported that the inclined rib arrangement with a downstream gap position shows higher improvement in heat transfer compared to that of the continuous inclined rib arrangement. In the recent study, Aharwal et al. [16] they are investigated to inclined rib with a gap provision so as to allow release of secondary flow and primary flow through the gap thereby creating local turbulence. They are investigation for the range of Reynolds number as 3000–18,000, aspect ratio as 5.84, relative roughness pitch as 10 and angle of attack as 60°. Gap width (g/e) and gap position (d/W) were in range of 0.5–2 and 0.1667–0.667 respectively. Higher enhancement in Nusselt number and friction factor was obtained as 2.59 and 2.87 times that of smooth plate respectively. Thermo hydraulic performance was obtained to be higher for relative gap width of 1.0 and relative gap position of 0.25. Aharwal et al. [17] has done an experimental investigation on heat transfer and friction factor characteristics utilizing integral inclined discrete square ribs on plate of a solar air heater. Comes about how that most extreme addition in nusselt number (Nu) is seen at a relative gap position of 0.25 for relative gap width of 1.0, p/e of 8.0, an of 60° and e/D of 0.037. Based upon gathered information, connections were produced for Nusselt number and friction factor.

In view of the above, it can be stated that discrete inclined or V-shaped rib arrangement yields better performance as compared to continuous rib arrangement. However, investigations have not been carried out so far to see the effect of gap width between the rib elements to form the discrete rib.

The present investigation was therefore taken up to seen the effect of gap in inclined ribs with a gap in staggered. In the current research work, experimental investigation on the performance analysis of solar air heater duct roughened with inclined ribs with a gap in a staggered roughness arrangement on absorber plate has been carried out. The flow Reynolds number has been varied between 3000 and 14,000. The variations of Nusselt number and friction factor as a function of roughness parameters including gap position have been evaluated to examine the thermo-hydraulic performance of the system to ascertain the benefit of this selected roughness geometry.

2. EXPERIMENTAL SETUP

The experimental schematic diagrams set-up including the test section is shown in Fig.1. The flow system consists of an entry section, test section, an exit section, a flow meter and a centrifugal blower. The duct is of size 2042 mm x 200 mm x 20 mm (dimension of inner cross-section) and is constructed from wooden panels of 25mm thickness. The test section is of length 1500 mm

International Journal of Engineering Technology Science and Research
IJETSR
www.ijetsr.com
ISSN 2394 – 3386
Volume 5, Issue 1
January 2018

(33.75D_h).The entry and exit lengths were 192 mm (7.2D_h) and 350 mm (12D_h), respectively. A short entrance length (L/D_h=7.2) was chosen because for a roughened duct the thermally fully developed flow is established in a short length 2-3 hydraulic diameter For the turbulent flow regime, ASHRAE standard 93-77 [18] recommends entry and exit length of 5√WH and 2.5√WH, respectively.

In the exit section after 116 mm, three equally spaced baffles are provided in an 87 mm length for the purpose of mixing the hot air coming out of solar air duct to obtain a uniform temperature of air (bulk mean temperature) at the outlet.

An electric heater having a size of 1500 mm x 216 mm was fabricated by combining series and parallel loops of heating wire Mica- sheet of 1mm is 'placed between the electric heater and absorber plate. This mica sheet acts as an insulator between the electric heater and absorber plate (Aluminum plate).The heat flux may be varied from 0 to 1000 W/m^2 by a variac across it.

The outside of the entire set-up, from the inlet to the orifice plate, is insulated with 25 mm thick polystyrene foam having a thermal conductivity of 0.037 W/m-K. The heated plate is a 5 mm thick aluminum plate with integral rib-roughness formed on its rear side and this is forms the top broad wall of the duct, while the bottom wall is formed by 5 mm aluminum plate and 25 mm wood with insulation below it. The top sides of the entry and exit sections of the duct are covered with smooth faced 8 mm thick plywood.

The mass flow rate of air is measured by means of a calibrated orifice meter connected with an inclined manometer, and the flow is controlled by the control valves provided in the lines. The orifice plate has been designed for the flow measurement in the pipe of inner diameter of 53 mm, as per the recommendation of Preobrazhensky [19]. The orifice plate is fitted between the flanges, so aligned that it remains concentric with the pipe.

The length of the circular GI pipe provided was based on pipe diameter d_1, which is a minimum of 10 d_1 on the upstream side and 5 d_1 on the downstream side of the orifice plate as recommended by Ehlinger [20].

In the present work of experimental set-up we used 1000 mm (13 d_1) pipe length on the upstream side and 700 mm (9 d_1) on the downstream side. The calibrated copper-constant 0.3 mm (24 SWG) thermocouples were used to measure the air and the heated plate temperatures at different locations. The location of thermocouples on the heated wall is shown in Fig.2. A digital Data-Tracker and compute is used to indicate the output of the thermocouples in^{0}C.

The pressure drops a cross the test section was measured by a micro-manometer. It is an open flow loop that consists of a test duct with entrance & exit sections, a blower, control valve, orifice plate and various devices for measurement of temperature & fluid head.

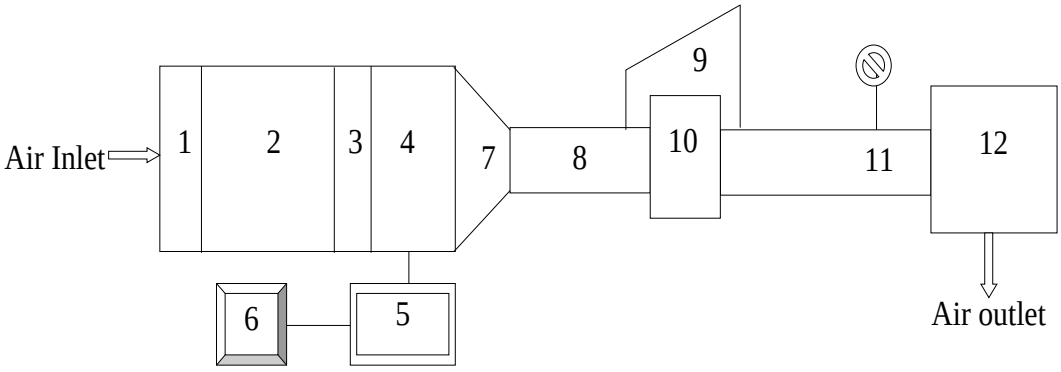

(1) Inlet Section, (2) Test Section, (3) Mixing Section, (4) Exit Section, (5) Data Tracker, (6) Computer, (7) Transition Section, (8) G.I. Pipe, (9) Inclined U-Tube Manometer, (10) Orifice Meter, (11) Control Valve, (12) Blower.

Fig.1. Schematic diagram of experimental setup.

International Journal of Engineering Technology Science and Research
IJETSR
www.ijetsr.com
ISSN 2394 – 3386
Volume 5, Issue 1
January 2018

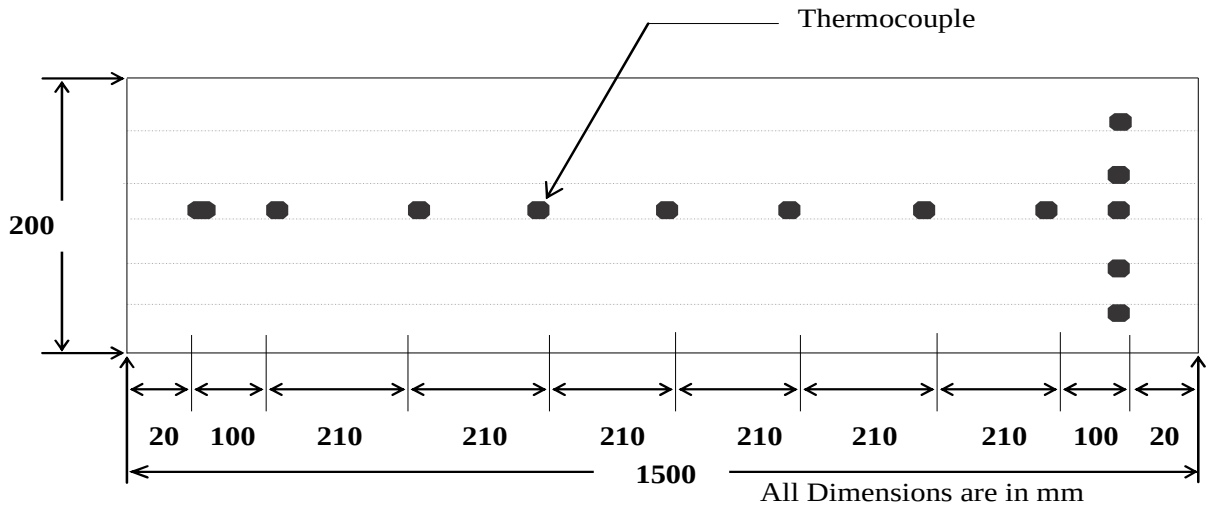

Fig.2. Position of thermocouples on absorbing plate (Test length).

3. ROUGHNESS GEOMETRY AND RANGE OF PARAMETERS

The value of system and working parameters of this experimental investigation are recorded in Table no. 1. The relative roughness pitch (P/e) value is selected as 8.0, based on the optimum value of this parameter announced in the Literature [16, 17]. Similarly, the value of the approach is picked at angle of attack (α) 90°, to achieve higher enhancement of heat transfer. The arrangements of ribs on the absorber plate are appeared in Fig. 3(a, b) in order to investigate the effect.

TABLE NO. 1

Value of Parameter

S.No.	Parameters	Value
1	Reynolds number (Re)	3000-14000
2	Relative roughness pitch (p/e)	8.0
3	Rib height (e)	2mm
4	Rib width (b)	2mm
5	Hydraulic diameter (D_h)	44.44
6	Relative roughness height (e/Dh)	0.045
7	Gap width (g)	2mm
8	Duct aspect ratio (W/H)	8
9	Angle of attack (α)	90°
10	Heat flux (I)	900W/m^2
11	Relative gap position (dt/W & dl/W)	0.3 & 0.1
12	Relative gap width (g/e)	1.0

International Journal of Engineering Technology Science and Research
IJETSR
www.ijetsr.com
ISSN 2394 – 3386
Volume 5, Issue 1
January 2018

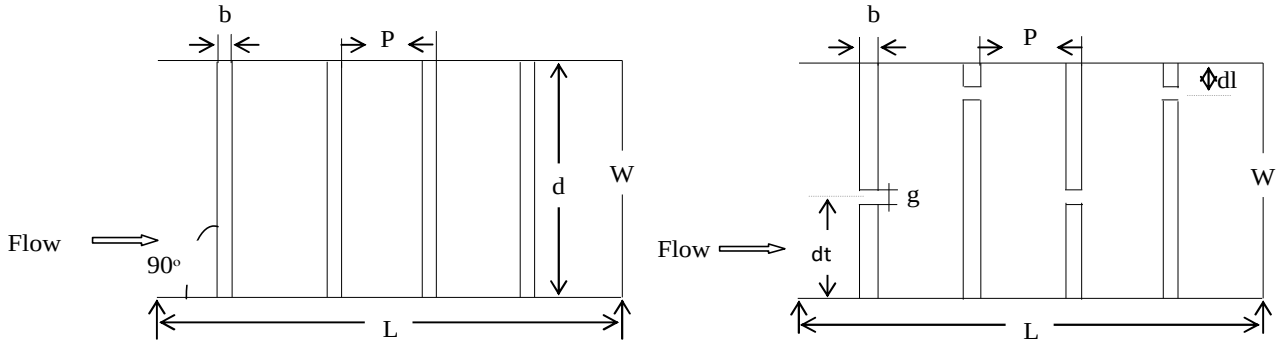

(a) Continuous Rib (b) dt/W & dl/W = 0.3 & 0.1

Fig.3. (a,b) Variation of with and without gap position at angle of attack (α) 90° in a inclined ribs with a gap in staggered arrangements.

4. DATA REDUCTION

i. Average Plate Temperature

Average plate data temperature is determined as follows:

$$T_p = (T_{P1} + T_{P2} + T_{P3} + T_{P4} + T_{P5} + T_{P6})/6 \quad (1)$$

ii. Average Outlet Air Temperature

Average air temperature is determined as:

$$T_o = (T_{O1} + T_{O2} + T_{O3} + T_{O4} + T_{O5})/5 \quad (2)$$

iii. Air properties at bulk air temperature

Corresponding to average air temperature

Specific heat of air

$$C_p = 1006 \times (T_f/293)^{0.0} \quad J\,kg^{-1}K^{-1} \quad (3)$$

Dynamics viscosity of air

$$\mu = 1.81 \times 10^{5}(T_f/293)^{0.7} \quad N\,s\,m^{-2} \quad (4)$$

Thermal conductivity of air

$$\kappa = 0.257(T_f/293)^{0.8} \quad W\,m^{-1}K^{-1} \quad (5)$$

Density of air

$$\rho = P_a/R_f\,k \quad kg/m^3 \quad (6)$$

Means bulk air temperature of air

$$T_f = (T_i - T_o)/2 \quad (7)$$

Where,

C_p= Specific heat of air, J kg^{-1} K^{-1}

μ = Dynamics viscosity of air, Ns m^2

κ = Thermal conductivity of air, W $m^{-1}K^{-1}$

ρ = Density of air, Kg/m^3

P_a = Atmospheric pressure

R = Characteristic of gas constant

(R=287.045 J kg^{-1} K^{-1})

T_f = mean bulk air temperature, °C

iv. Pressure Drop Calculation

Pressure drop measurement across the orifice plate by using the following relationship:

$$\Delta P_0 = \Delta h \times 9.81 \times \Delta\rho \quad (8)$$

Where,

ΔPo = Pressure diff. across orifice meter

Δρm = Density of the manometer fluid

Δ h = Difference of liquid head in U-tube manometer, m

v. Mass Flow Measurement

Mass flow rate of air has been determined from pressure drop measurement across the orifice plate by using the following relationship:

$$\dot{m} = C_d \times A_o \times [2\rho\Delta P_o/(1-\beta^4)]^{0.5} \quad (9)$$

Where,

ṁ = Mass flow rate, kg / sec.

C_d = Coefficient of discharge of orifice i.e. 0.61

A_0 = Area of orifice plate, m^2

ρ = Density of air in Kg/m^3

β = Ratio of orifice diameter to pipe diameter.

(β =d_o / d_p) i.e. 26.5/53 = 0.5

International Journal of Engineering Technology Science and Research
IJETSR
www.ijetsr.com
ISSN 2394 – 3386
Volume 5, Issue 1
January 2018

vi. Velocity Measurement:

$V = \dot{m}/\rho$ (10)

Where,

ṁ = Mass flow rate, kg / sec

ρ = Density of air in Kg/m^3

H = Height of the duct in m

W = Width of the duct, m

vii. Reynolds Number

The Reynolds number for flow of air in the duct is calculated from:

$R = V_h/\nu$ (11)

Where,

ν = Kinematics viscosity of air at average fluid temperature

$D_h = 4W/2(W + H)$ (12)

viii. Heat Transfer Coefficient

Heat transfer rate, Qa to the air is given by:

$Q_a = \dot{m}C_p(T_o - T_i)$ (13)

Where,

ṁ = Mass flow rate, kg / sec

C_p = Density of air in Kg/m^3

T_o = outlet temperature of air

T_i = Inlet temperature of air

The heat transfer coefficient for the heated test section has been calculated from:

$h = \frac{Qa}{Aa}(T_p - T_f)$ (14)

Where,

A_p = the heat transfer area assumed to be the corresponding smooth plate area.

ix. Nusselt Number

Heat Transfer Coefficient has been used to determine the Nusselt number defined as;

$N = \frac{hD_h}{K}$ (15)

Where,

k = the thermal conductivity of the air at the mean air temperature

D_h = the hydraulic diameter based on entire wetted perimeter.

x. Friction Factor

The friction factor was determined from the flow velocity, V‟ and the head loss „Δhd‟ measured across the test section length of 1m using the Darcy– Weisbach equation as

$f = 2[(\Delta P)_d]\, D_h/4\rho\, fV^2$ (16)

Where,

ΔP = Pressure drop in N/m^2 for 1.36m length, L_f .of the duct

Dh = the hydraulic diameter based on entire wetted perimeter

xi. Thermo Hydraulic Performance:

Thermo hydraulic performance is calculated by

$T_{hp} = (N_r/N_s)/(f_r/f_s)^{1/3}$ (17)

5. VALIDATION OF EXPERIMENTAL DATA

The Estimation of Nusselt number and friction factor obtained from experimental data for smooth duct have been compared with the estimation obtained from Dittus–Boelter equation for the Nusselt number and modified Blasius equation for the friction factor. The Nusselt number for a smooth rectangular duct is given by the Dittus–Boelter equation as

$N_s = 0.023R^{0.8}P^{0.4}$ (18)

The friction factor for a smooth rectangular duct is given by the modified Blasius equation as

$f_s = 0.85R^{-0.2}$ (19)

The comparison of the experimental and estimated values of the Nusselt number and friction factor as a function of the Reynolds number is shown in Figure (4) and Figure (5), respectively. The average deviation of experimental estimation of the Nusselt number is ± **1.02% from** the estimation predicted by Equation (18), and the average deviation of Experimental estimation of the measured friction factor is **± 0.09%** from the estimation predicted by Equation (19).Thus, reasonably good agreement between the two sets of values ensures the accuracy of the data being collected with the experimental setup.

International Journal of Engineering Technology Science and Research
IJETSR
www.ijetsr.com
ISSN 2394 – 3386
Volume 5, Issue 1
January 2018

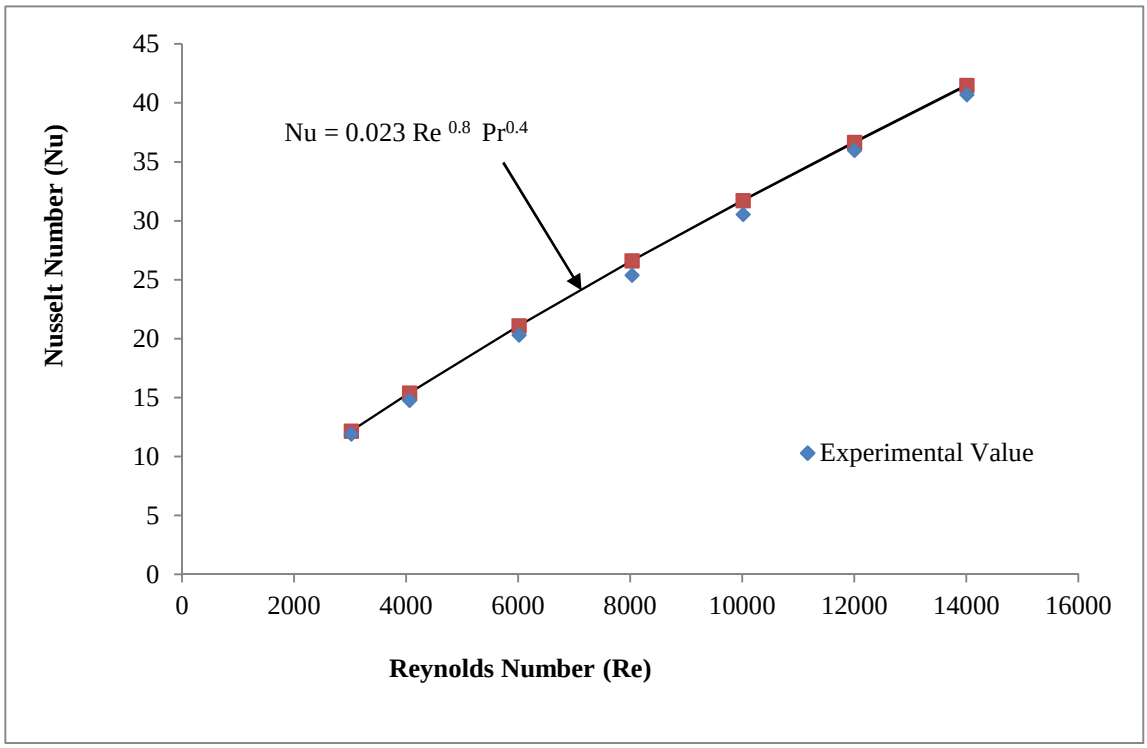

Figure (4) Comparison of experimental and estimated values of Nusselt number of smooth duct.

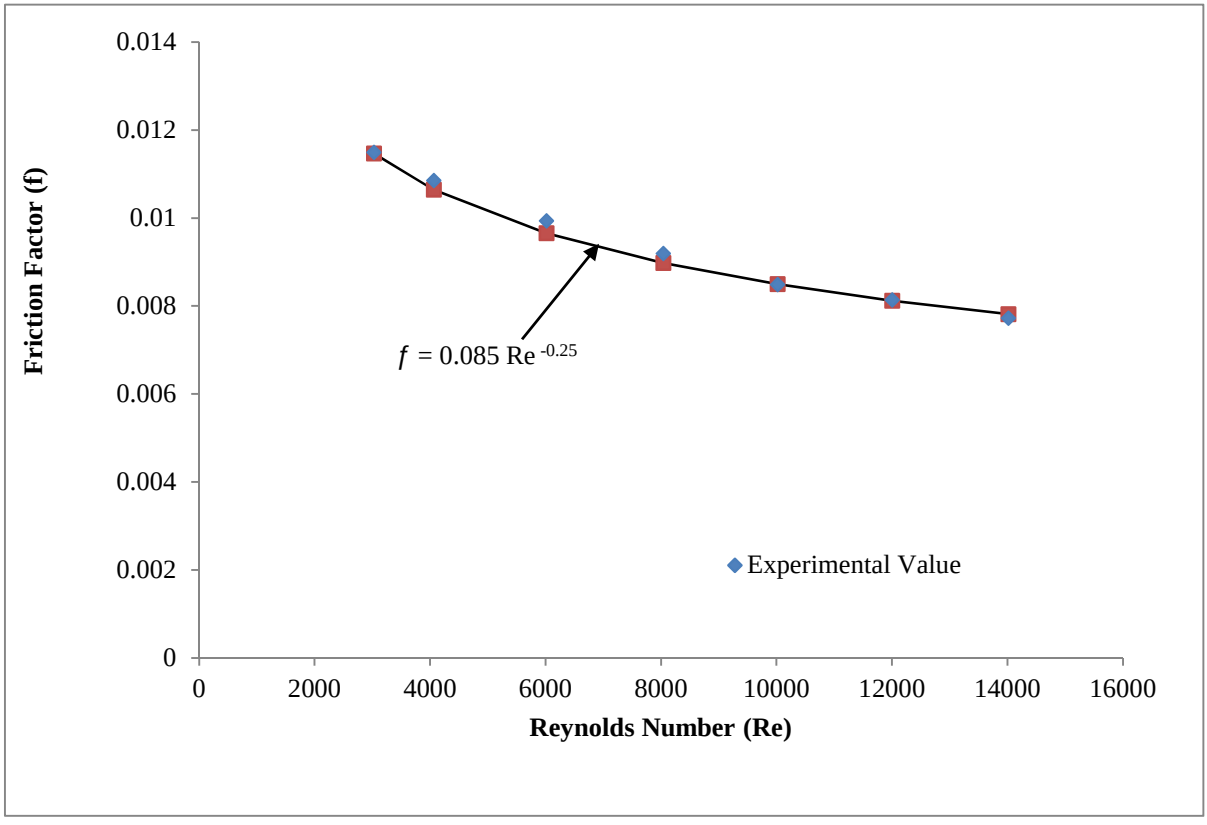

Figure (5) Comparison of experimental and estimated values of friction factor of smooth duct.

International Journal of Engineering Technology Science and Research
IJETSR
www.ijetsr.com
ISSN 2394 – 3386
Volume 5, Issue 1
January 2018

6. RESULTS AND DISCUSSION

The effect of various flow and roughness parameters on heat transfer characteristics for flow of air in artificial roughness due to a gap in an staggered inclined discrete rib arrangement in a Rectangular ducts of relative roughness height in the present investigation are discussed below. Results have also been compared with those of smooth ducts under similar flow conditions to seen the improvement in heat transfer coefficient.

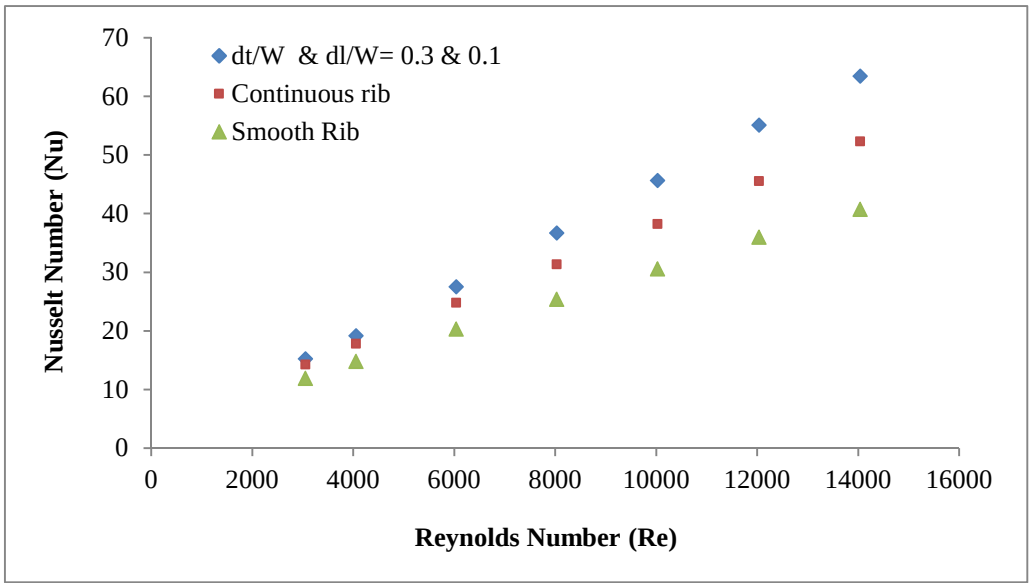

Figure (6) Variation of Nusselt number with Reynolds number.

The variation of Nusselt number with Reynolds number is shown in Figure (6). It is seen that the value of Nusselt number is increases with increases in Reynolds number. The value of Nusselt number is varies from 15 to 63 in the range of Reynolds number 3000-14000. The higher value of Nusselt number is observe for rib with gap roughness arrangement (dt/W & dl/W = 0.3 & 0.1). This may due to the fact that the presence of gap produces more turbulence, which improves the heat transfer.

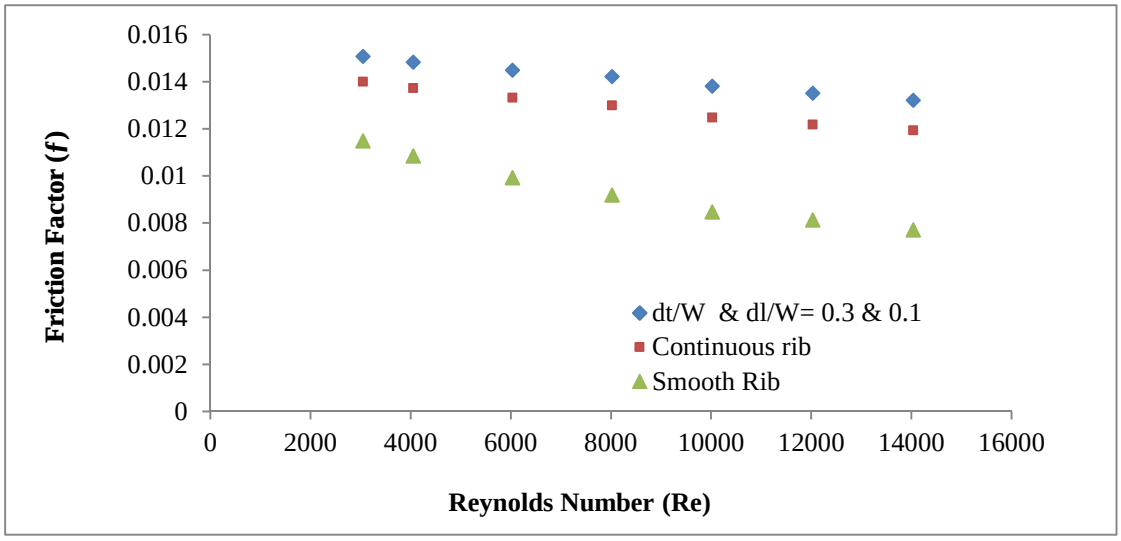

Figure (7) Variation of Friction factor with Reynolds number.

International Journal of Engineering Technology Science and Research
IJETSR
www.ijetsr.com
ISSN 2394 – 3386
Volume 5, Issue 1
January 2018

The variation of friction factor with Reynolds number is shown in Figure (7). It is seen that the value of friction factor decreases with increase in Reynolds number. This may be due to the fact that as the Reynolds number increases, the thickness of boundary layer decreases therefore, friction factor decreases with increase in Reynolds number. The higher value of friction factor is observe for rib with gap roughness arrangement, whereas it's lower value is observed for smooth duct. The value of friction factor of continuous rib roughness arrangement is lower than that of the rib with gap roughness arrangement (dt/W & dl/W = 0.3 & 0.1).

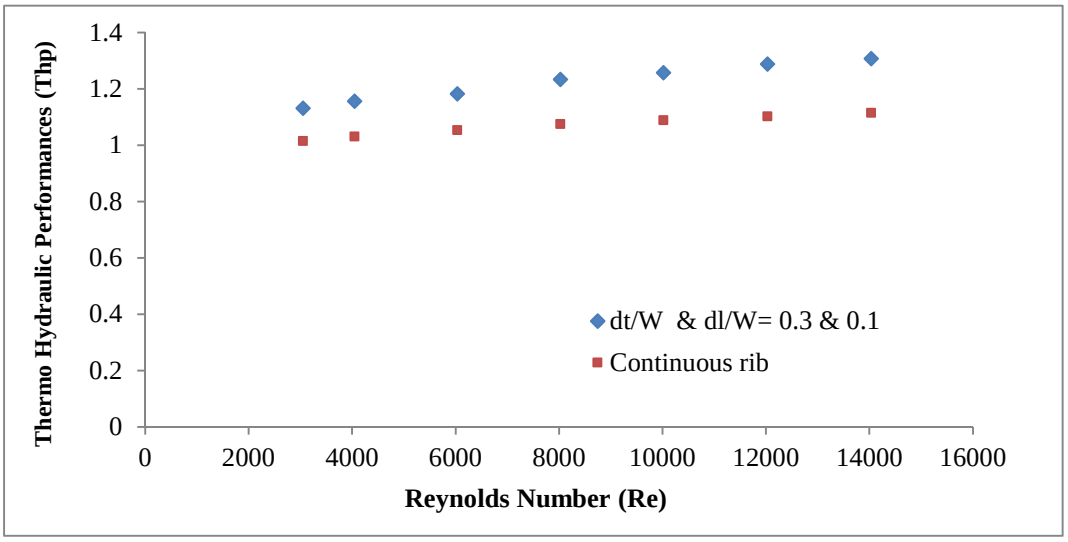

Figure (8) Variations of Thermo Hydraulic performances with Reynolds number.

The variation of thermo hydraulic performance with Reynolds number is shown in Figure (8). It is seen that the value of Reynolds number increases with increase in thermo hydraulic performance and after attaining higher value, thermo hydraulic performance decreases with increase in Reynolds number. The value of thermo hydraulic performance is varies from 1.13 to 1.30 in the range of Reynolds number 3000-14000. The higher value of thermo hydraulic performance is observed for the rib with gap roughness arrangement (dt/W & dl/W = 0.3 & 0.1) and minimum value is achieved for smooth rib.

7. CONCLUSION

Based on this experimental investigation on angle of attack at (α) 90° - inclined ribs with and without a gap in staggered arrangement roughened ducts, the Following conclusions can be drawn.

a) The value of Nusselt number increases with increase in Reynolds number. The higher value of Nusselt number is observe for inclined ribs with gap in staggered roughness arrangement because the presence of inclined ribs with gap in staggered roughness increases the level of turbulence, which cause enhancement in heat transfer.

b) The value of friction factor decrease with increase in value of Reynolds number. The higher value of friction factor is observed for inclined ribs with gap in staggered roughness arrangement. The value of friction factor of continuous rib roughness arrangement is less than that of the inclined ribs with gap in staggered roughness arrangement.

c) It is observe that the value of thermo hydraulic performance parameter increase with increase in Reynolds number the maximum value of this parameter is observe for inclined ribs with gap in staggered roughness arrangement.

8. REFERENCES

[1] Varun, R.P. Saini, S.K. Singal, (2008) Investigation of thermal performance of solar air heater having roughness elements as a combination of inclined and transverse ribs on absorber plate, Renew. Energy l33, 1398-1405.

[2] A. Kumar, R.P. Saini, J.S. Saini, (2012) Experimental investigation on heat transfer and fluid

flow characteristics of air flow in a rectangular duct with Multi V-shaped rib with gap roughness on the heated plate, Sol. Energy 86 ,1733-1749.

[3] B.N. Prasad, Arun K. Behura, L. Prasad, (2014) Fluid flow and heat transfer analysis for heat transfer enhancement in three sided artificially roughened solar air heater, Sol. Energy 105, 27-35.

[4] D. Gupta, S.C. Solanki, J.S. Saini, (1997) Thermohydraulic performance of solar air heaters with roughened absorber plates, Sol. Energy 61, 33-42.

[5] S. Singh, S. Chander, J.S. Saini, (2011) Thermal and effective efficiency based analysis of discrete V down rib roughened solar air heaters, J. Renew. Sustain Energy 3, 023107-023126.

[6] M.K. Mittal, Saini RP. Varun, S.K. Singal, (2007) Effective efficiency of solar air heaters having different types of roughness elements on the absorber plate, Energy 32, 739-745.

[7] A. Layek, J.S. Saini, S.C. Solanki, (2007) Second law optimization of a solar air heater having chamfered rib-groove roughness on absorber plate, Renew. Energy 32, 1967-1980.

[8] M.K. Gupta, S.C. Kaushik, (2009) Performance evaluation of solar air heater for various artificial roughness geometries based on energy, effective and exergy efficiencies, Renew. Energy 34, 465-476.

[9] M.K. Gupta, S.C. Kaushik, (2009) Performance evaluation of solar air heater having expanded metal mesh as artificial roughness on absorber plate, Int. J. Therm. Sci. 48, 1007-1016.

[10] Lau SC, McMillin RD, Han JC., (1991) turbulent heat transfer and friction in a square channel with discrete rib turbulators. Trans ASME, J Turbo Machinery, 113:360–6.

[11] Lau SC, McMillin RD, Han JC., (1991) Heat transfer characteristics of turbulent flow in a square channel with angled rib. Trans ASME, J Turbo machinery 113:367–74.

[12] Han JC, Zhang YM., (1992) High performance heat transfers ducts with parallel broken and V- shaped broken ribs. Int. J Heat Mass Transfer, 35(2):513–23.

[13] Kiml R, Mochizuki S, Murata A., (2001) Effects of rib arrangements on heat transfer and flow behavior in a rectangular rib roughened passage. J Heat Transfer, 123:675–81.

[14] Cho HH, Wu SJ, Kwon HJ., (2000) Local heat/mass transfer measurement in a rectangular duct with discrete ribs. J Turbo machinery, 122: 579–86.

[15] Cho HH, Kim YY, Rhee DH, Lee SY, Wu SJ., (2003) the effect of gap position in discrete ribs on local heat/mass transfer in a square duct. J Enhanced Heat Transfer, 10(3):287–300.

[16] Aharwal, K.R., Gandhi, B.K., Saini, J.S., (2008). Experimental investigation on heat-transfer enhancement due to a gap in an inclined continuous rib arrangement in a rectangular duct of solar air heater. Renewable Energy, 33, 585–596.

[17] Aharwal, K.R., Gandhi, B.K., Saini, J.S., (2009). Heat transfer and friction characteristics of solar air heater ducts having integral inclined discrete ribs on absorber plate. Int. J. Heat M. Transfer 52, 5970–5977.

[18] ASHARAE Standard (93–77). Method of testing to determine the thermal performance of Solar Air Heater, New York 1997; 1–34.

[19] Preobrazhensky VP., (1980) Measurement and Instrumentation in Heat Engineering [English translation], vol. 2. Moscow: Mir Publisher.

[20] Ehlinger AH**.,** **(**1950) Flow of air and gases. In: Salisbury JK, editor, Kent's Mechanical Engineers Hand- book, Power Volume. New York: Wiley, 1.101.21.